AGU PUBLICATIONS

Geophysical Research Letters

RESEARCH LETTER
10.1002/2014GL061450

Key Points:
- Upwelling variations off southern Indonesia over the past 2000 years
- Upwelling was strong during Little Ice Age and weak during Medieval Warm Period
- ENSO may have contributed to changes in upwelling off southern Indonesia

Supporting Information:
- Readme
- Figure S1
- Figure S2

Correspondence to:
S. Steinke,
ssteinke@marum.de

Citation:
Steinke, S., M. Prange, C. Feist, J. Groeneveld, and M. Mohtadi (2014), Upwelling variability off southern Indonesia over the past two millennia, *Geophys. Res. Lett.*, *41*, 7684–7693, doi:10.1002/2014GL061450.

Received 6 AUG 2014
Accepted 22 OCT 2014
Accepted article online 27 OCT 2014
Published online 12 NOV 2014

Upwelling variability off southern Indonesia over the past two millennia

Stephan Steinke[1], Matthias Prange[1], Christin Feist[1], Jeroen Groeneveld[1], and Mahyar Mohtadi[1]

[1]MARUM–Center for Marine Environmental Sciences, University of Bremen, Bremen, Germany

Abstract Modern variability in upwelling off southern Indonesia is strongly controlled by the Australian-Indonesian monsoon and the El Niño–Southern Oscillation, but multidecadal to centennial-scale variations are less clear. We present high-resolution records of upper water column temperature, thermal gradient, and relative abundances of mixed layer- and thermocline-dwelling planktonic foraminiferal species off southern Indonesia for the past two millennia that we use as proxies for upwelling variability. We find that upwelling was generally strong during the Little Ice Age (LIA) and weak during the Medieval Warm Period (MWP) and the Roman Warm Period (RWP). Upwelling is significantly anticorrelated to East Asian summer monsoonal rainfall and the zonal equatorial Pacific temperature gradient. We suggest that changes in the background state of the tropical Pacific may have substantially contributed to the centennial-scale upwelling trends observed in our records. Our results implicate the prevalence of an El Niño-like mean state during the LIA and a La Niña-like mean state during the MWP and the RWP.

1. Introduction

Along the southern coasts of Java, southern Sumatra, and the Lesser Sunda Islands (Nusa Tenggara), southeasterly winds from Australia generate intensive coastal upwelling during austral winter (June–September), bringing cooler nutrient-rich waters to the surface resulting in enhanced marine biological productivity [e.g., *Hendiarti et al.*, 2004; *Susanto et al.*, 2006; *Ningsih et al.*, 2013]. Conditions are reversed during the northwest austral summer monsoon (December to February). Upwelling is generally absent during this season as well as during the transitional period of the monsoon (March–May). Modern interannual variability in upwelling is strongly correlated with the El Niño–Southern Oscillation (ENSO) and the Indian Ocean Dipole (IOD) [e.g., *Susanto et al.*, 2001; *Sprintall et al.*, 2003; *Susanto and Marra*, 2005]. El Niño (and positive IOD) years are associated with anomalously strong southeasterly winds that enhance coastal upwelling during boreal summer/austral winter. In contrast, during La Niña (and negative IOD) years, upwelling strength is reduced due to westerly wind anomalies resulting in uniformly high sea surface temperature (SST) along the southern coasts of Java, southern Sumatra, and the Lesser Sunda Islands [e.g., *Susanto et al.*, 2001].

On glacial-interglacial timescales, upwelling off southern Java changed in concert with upwelling in the Arabian Sea most likely through variations in the strength of large-scale cross-equatorial boreal summer/austral winter monsoon winds in response to Northern Hemisphere summer insolation [*Mohtadi et al.*, 2011a]. However, high-resolution records reflecting the multidecadal to centennial-scale dynamics of upwelling strength off southern Indonesia for the late Holocene, in particular for the last two millennia, are still missing. These are crucial for a deeper understanding of the natural variability of the atmospheric/monsoonal circulation system in the context of present and future climate change. Reconstructing climate variability of the past two millennia thus has become a primary interest to the paleoclimate science community because this timescale is highly relevant to better understand the influence of external forcings and internal climate variability as well as to distinguish between natural and human-induced changes on the global climate system [e.g., *Masson-Delmotte et al.*, 2013; *PAGES 2 K Consortium*, 2013].

In this study, we present high-resolution records of upper water column temperature and thermal gradient (i.e., upper water column stratification; depth of thermocline) for the last 2000 years from a sediment archive collected offshore northwest Sumba Island (Lesser Sunda Islands; southern Indonesia) that we use as proxies for changes in upwelling intensity (Figure 1). We reconstruct upper water temperatures based on shell Mg/Ca of the planktonic foraminiferal species *Globigerina bulloides* and *Pulleniatina obliquiloculata*. Based on measured Mg/Ca values temperatures in core tops, *G. bulloides* and *P. obliquiloculata* records in the

©2014. American Geophysical Union. All Rights Reserved.

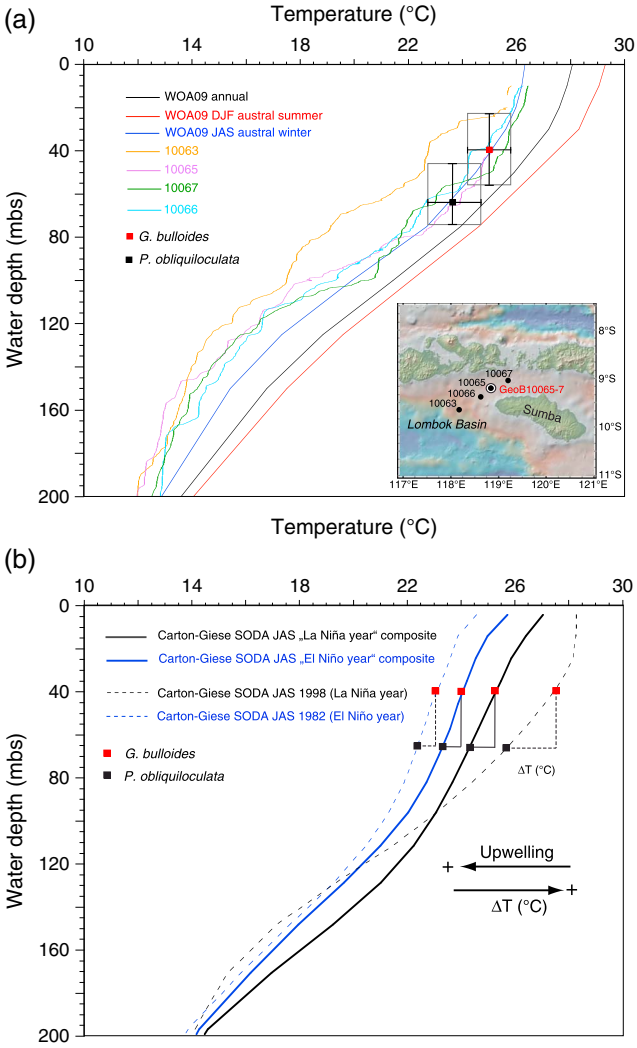

Figure 1. (a) Temperature profiles of the upper 200 m in the Lombok Basin based on WOA09 [*Locarnini et al.*, 2010] and R/V *Sonne* cruise SO-184 conductivity-temperature-depth profiles acquired in early September 2005 at stations 10063 (orange line), 10065 (purple line), 10067 (green line), and 10066 (light blue line) [*Mohtadi et al.*, 2007]. Solid black line: WOA09 annual mean temperatures; red solid line: WOA09 austral summer temperatures; blue solid line: WOA09 austral winter temperatures (JAS). Squares indicate temperatures, calculated from shell Mg/Ca ratios for *G. bulloides* (red) and *P. obliquiloculata* (black) from core top samples. Lines and boxes denote the range of the calculated temperatures in different samples [*Mohtadi et al.*, 2011b] and the related depth range of both planktonic foraminifera species. Mg/Ca temperatures are calculated using species-specific equations of *Cléroux et al.* [2008] for *P. obliquiloculata* and *Elderfield and Ganssen* [2000] for *G. bulloides*. Based on these measured Mg/Ca temperatures in core top samples, *G. bulloides* and *P. obliquiloculata* record mean calcification temperatures at ~40 m and ~65 m water depth during the austral winter (upwelling) season in the Lombok Basin, respectively [*Mohtadi et al.*, 2009, 2011b], the location of gravity core GeoB10065-7 is also indicated, the map in Figure 1a has been created using GeoMapApp available under www.geomapapp.org; (b) Austral winter (JAS) composite El Niño years (1963, 1965, 1972, 1982, 1987, 1991, 1997, and 2002; blue line) and La Niña years (1964, 1970, 1971, 1973, 1975, 1984, 1985, 1988, 1998, and 1999; black line) temperature depth profiles and temperature depth profiles for the year 1982 (El Niño year; blue broken line) and 1998 (La Niña year; black broken line) of the upper 200 m in the Lombok Basin based on Carton-Giese simple ocean data assimilation (SODA) [*Carton and Giese*, 2008]. Assuming a stable depth habitat for *G. bulloides* and *P. obliquiloculata* of ~40 m and ~65 m water depth, stronger upwelling, i.e., an El Niño year is associated with a lower temperature difference (ΔT°C) between *G. bulloides* and *P. obliquiloculata*, whereas periods of reduced upwelling, i.e., a La Niña year, are associated with a higher ΔT°C. A lower (higher) temperature difference between both species is, therefore, generally interpreted to reflect stronger (weaker; more stratified upper water column; deeper mixed layer) upwelling and a shallow (deepened) thermocline in the tropical eastern Indian Ocean.

©2014. American Geophysical Union. All Rights Reserved.

Lombok Basin represent mean calcification temperatures at ~40 m and ~65 m water depth during the austral winter season [*Mohtadi et al*., 2011b] (Figure 1a). This is confirmed by sediment trap flux data off southern Java, which show highest species-specific fluxes for *G. bulloides* and *P. obliquiloculata* during the austral winter/upwelling season [*Mohtadi et al*., 2009]. During El Niño years, the species-specific fluxes for *G. bulloides* and *P. obliquiloculata* in the upwelling season (July-August-September (JAS)) are higher compared to La Niña years which is in agreement with enhanced upwelling during El Niño years [*Mohtadi et al*., 2009]. We use the difference in Mg/Ca-based temperatures (ΔT°C) of these species to infer changes in upper water column structure during the austral winter/upwelling season. An essential precondition of this approach is that planktonic foraminifera have a relatively stable depth habitat [e.g., *Steinke et al*., 2010, 2011]. Most important for our approach is that interannual variability in upwelling in our study area due to ENSO is not associated with a shift in seasonality of *G. bulloides* and *P. obliquiloculata* [*Mohtadi et al*., 2009]. Accordingly, stronger upwelling, e.g., during El Niño years, is associated with a lower temperature difference (ΔT°C) between *G. bulloides* and *P. obliquiloculata*, whereas periods of reduced upwelling, e.g., during La Niña years, are characterized by a higher ΔT°C (Figure 1b). Thus, a lower (higher) temperature difference between both species is generally interpreted to reflect stronger (weaker; more stratified upper water column; deeper mixed layer) local upwelling and a shallow (deepened) thermocline in the tropical eastern Indian Ocean. Reconstructing the relative state of the upper water column structure thus represents a sensitive diagnostic variable of past changes in thermocline depth and upwelling strength [*Mohtadi et al*., 2011b]. In addition, we use the relative abundances of mixed layer-dwelling planktonic foraminifera (e.g., *Globigerinoides ruber*, *Globigerinoides sacculifer*, *Globigerinita glutinata*) and thermocline-dwelling species (e.g., *P. obliquiloculata*, *Globorotalia menardii*, *Neogloboquadrina dutertrei*) as a proxy for thermocline depth and austral winter upwelling strength. Previous studies suggest that thermocline shoaling is associated with a decrease in the abundance of mixed layer-dwelling species, while the thermocline-dwelling species increase in abundance [e.g., *Ravelo et al*., 1990].

2. Material and Methods

Gravity core GeoB10065-7 (9°13.39′S; 118°53.58′E; 1296 m water depth; core length 9.75 m) was recovered from the eastern Lombok Basin northwest off Sumba Island during the R/V *Sonne* SO-184 "PABESIA" expedition in 2005 (Figure 1a). The sediments consist exclusively of nannofossil ooze with a turbidite occurring at 37–40 cm depth in the core. The chronology of the top 4.4 m of gravity core GeoB10065-7, which spans the last ~2000 years is based on excess ^{210}Pb, an anthropogenic fallout radionuclide ^{241}Am and 17 Accelerator Mass Spectrometry radiocarbon dates. Details about the age model of core GeoB10065-7 can be found in *Steinke et al*. [2014]. Sedimentation rates at site GeoB10065-7 range between 0.11 cm/yr and 0.35 cm/yr [*Steinke et al*., 2014].

Mg/Ca analyses on *G. bulloides* and *P. obliquiloculata* were performed on a subset of samples with 1 to 3 cm spacing (~4–16 year per sample). For each sample, approximately 30 specimens of *G. bulloides* and *P. obliquiloculata* were picked out of the 250–350 μm size fraction of the upper 4.4 m of core GeoB10065-7. Foraminiferal tests were cleaned following the cleaning protocol developed by *Barker et al*. [2003] and analyzed with an inductively coupled plasma optical emission spectroscopy (ICP-OES) (Agilent Technologies, 700 Series with autosampler ASX-520 Cetac and micronebulizer) at the MARUM–Center for Marine Environmental Sciences, University of Bremen, Germany. Instrumental precision of the ICP-OES was monitored by analysis of an in-house standard solution with a Mg/Ca of 2.93 mmol/mol after every five samples (long-term standard deviation of 0.026 mmol/mol). To allow interlaboratory comparison we analyzed an international limestone standard (ECRM752–1) with a reported Mg/Ca of 3.75 mmol/mol [*Greaves et al*., 2008]. The long-term average of the ECRM752–1 standard, which is routinely analyzed twice before each batch of 50 samples in every session, is 3.78 mmol/mol (1σ = 0.066 mmol/mol). Analytical precision based on three replicate measurements of each sample for *G. bulloides* and *P. obliquiloculata* was 0.07% (n = 420) and 0.11 mmol/mol (n = 189) for Mg/Ca, respectively. Replicate measurements (repicked and separately cleaned) of *G. bulloides* samples (n = 15) and *P. obliquiloculata* samples (n = 9) revealed a standard deviation of 0.17 mmol/mol and 0.11 mmol/mol, respectively. The Mg/Ca ratios are not affected either by the occurrence of synsedimentary and postdepositional precipitated Mn oxide and Mn-rich carbonate coatings, or by postdepositional partial dissolution. Temperature (T in °C) estimates for *G. bulloides* were obtained by using the species-specific equation of *Elderfield and Ganssen* [2000] (Mg/Ca (mmol/mol) = 0.81 exp (0.081 × T))

©2014. American Geophysical Union. All Rights Reserved.

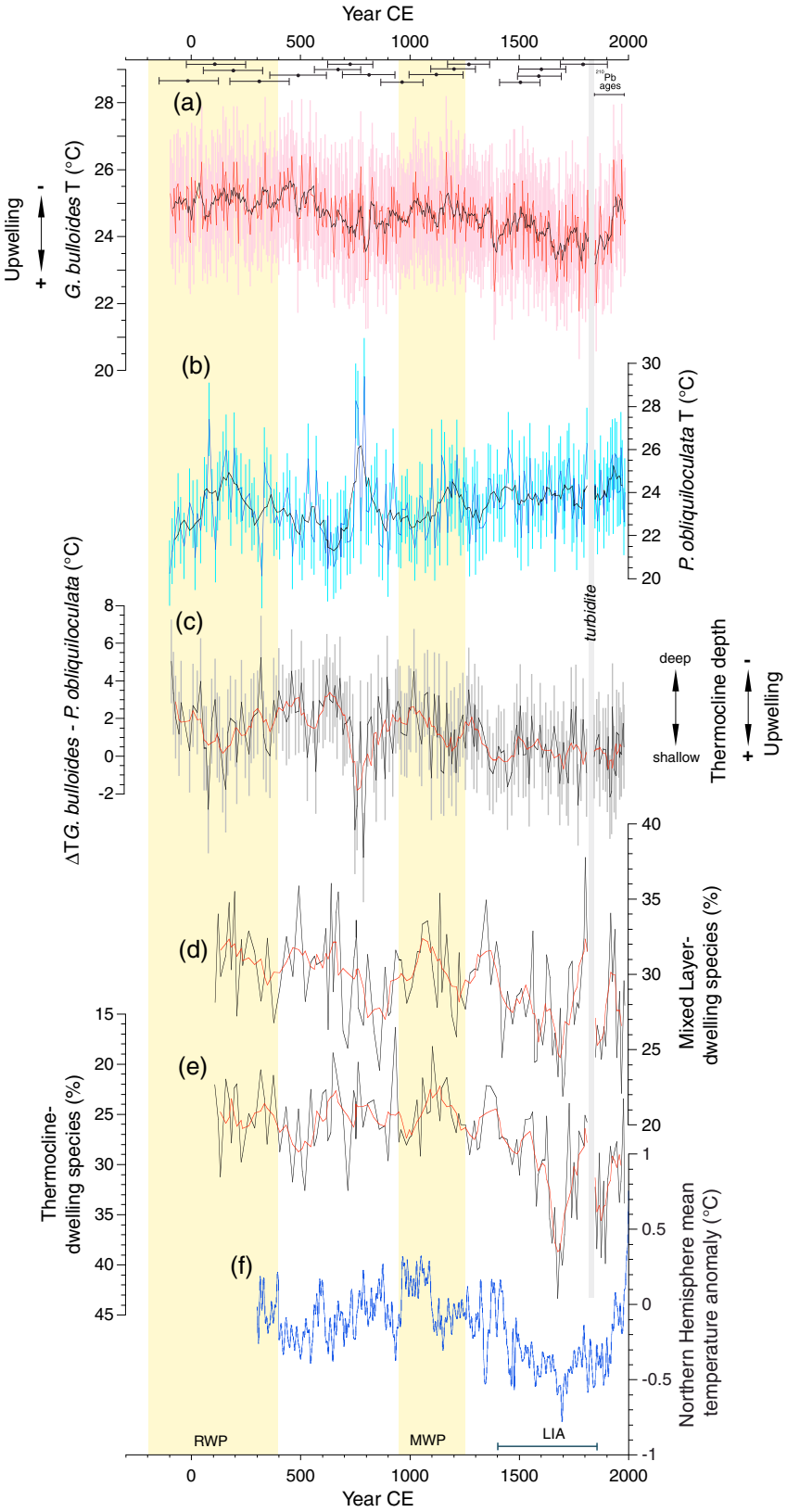

Figure 2

©2014. American Geophysical Union. All Rights Reserved.

and for *P. obliquiloculata* by using the equation of *Cléroux et al.* [2008] (Mg/Ca (mmol/mol) = 0.78 exp (0.052 × T)). We selected these calibration equations because the derived core top temperatures were closest to modern seasonal observational values (WOA09) [*Locarnini et al.*, 2010]. Furthermore, the regional Mg/Ca temperature relationship of *G. bulloides* and *P. obliquiloculata* is best explained by these calibration equations [*Mohtadi et al.*, 2011b]. The errors of the temperature reconstructions are estimated by propagating the errors introduced by the Mg/Ca measurements and the Mg/Ca temperature calibration (see *Mohtadi et al.* [2014] for details). The resulting errors are on average 1.56°C for the *G. bulloides* and *P. obliquiloculata* temperature estimates. Accordingly, the resulting error (Gaussian error propagation) for the ΔT estimates is on average 2.21°C (see also Figure 2).

Planktonic foraminiferal census counts have been generated from the >150 μm size fraction at 1–6 cm sample spacing (~5–30 years sample resolution). A minimum of 300 planktonic foraminifera from the size fraction >150 μm were counted in each of the 118 selected samples which guarantees a satisfactory statistical accuracy, as shown by *Van der Plas and Tobi* [1965]. For example, the 2σ error of a relative abundance of 20% on a 300 specimen count is less than 5%.

For the calculations of linear Pearson correlation coefficients *r* between two records, common time axes have been created by using 10 year overlapping 50 year wide bins. The 95% confidence intervals for the correlation coefficients were calculated using a nonparametric bootstrap method, where autocorrelation (i.e., serial dependence) has been taken into account [*Olaffsdottir and Mudelsee*, 2014].

3. Results and Discussion

3.1. Mg/Ca Paleothermometry, Upper Water Column Structure, and Faunal Analyses

Mg/Ca ratios of *G. bulloides* vary between 4.7 mmol/mol and 6.9 mmol/mol (Figure S1 in the supporting information). The estimated Mg/Ca water temperatures range from 21.8°C to 26.5°C. The reconstructed austral winter (upwelling season) upper thermocline water temperatures reveal several centennial-scale warm (~ 0–600 Common Era (C.E.), ~ 900–1300 C.E., and ~ 1900–1980 C.E.) and cold periods (~700–900 C.E. and ~ 1400–1850 C.E.). For that reason, we compare our *G. bulloides* based temperature record with the reconstructed Northern Hemisphere temperature change of *Mann et al.* [2008]. We find that the *G. bulloides* upper water temperature record correlates well ($r = 0.54$ with 95% confidence interval (0.33; 0.79)) with the documented European/North Atlantic climate anomalies including the Roman Warm Period (RWP; ~250 before the Common Era (B.C.E.) to 400 C.E.), the Medieval Warm Period (MWP; ~ 950–1250 C.E.), the Current Warm Period (~1850 C.E. to present), and the cold Little Ice Age (LIA; ~1400–1850 C.E.). The austral winter near-surface water temperature estimates suggest that the LIA was approximately 1–2°C colder than the late twentieth century (Figure 2a). Periods of lower austral winter near-surface water temperatures compared to the late twentieth century are interpreted to reflect stronger upwelling (see discussion below).

Mg/Ca ratios of *P. obliquiloculata* vary between 2.2 mmol/mol and 3.5 mmol/mol over the last 2000 years (Figure S1 in the supporting information). The estimated upper thermocline temperatures range from 19.7°C to 28.8°C (Figure 2b). The inferred upper thermocline water temperatures reveal a maximum of ~25°C around 750 C.E. After decreasing to ~22°C around 900 C.E., upper thermocline temperatures show a gradual increase to the late twentieth century (Figure 2b). In order to test how the choice of different calibration equations for *P. obliquiloculata* affects the upper thermocline temperature estimates, we also used the species-specific

Figure 2. Proxy records of core GeoB10065-7 for the last 2000 years: (a) Estimated temperatures derived from *Globigerina bulloides* shell Mg/Ca ratios (five-point moving average in black); (b) estimated temperatures derived from *Pulleniatina obliquiloculata* shell Mg/Ca ratios (five-point moving average in black); (c) thermal gradient reconstructions ($\Delta T_{G.\ bulloides\ -\ P.\ obliquiloculata}$; five-point moving average in red); (d) relative abundance of mixed layer-dwelling planktonic foraminifera species; (e) relative abundance of thermocline-dwelling planktonic foraminifera species (raw data in black and five-point moving average in red, reversed axis); and (f) Northern Hemisphere temperature anomaly record [*Mann et al.*, 2008]. Yellow bars indicate warm northern European/North Atlantic climate anomalies: Roman Warm Period (RWP) and Medieval Warm Period (MWP). LIA: Little Ice Age. Dots with horizontal bars plotted at the top indicate calendar ages with 2σ errors. Grey bar shows the position of a turbidite occurring at 37–40 cm depth in core of GeoB10065-7. Error bars in (Figure 2a; red), (Figure 2b; blue), and (Figure 2c; black) indicate 1σ errors. The errors of the temperature reconstructions were estimated by propagating the errors introduced by the Mg/Ca measurements and the Mg/Ca temperature calibration [see *Mohtadi et al.*, 2014]. The resulting errors are on average 1.56°C for the *G. bulloides* and *P. obliquiloculata* temperature estimates. Accordingly, the resulting error (Gaussian error propagation) for the ΔT estimates is on average 2.21°C.

©2014. American Geophysical Union. All Rights Reserved.

equations of *Anand et al.* [2003] (Figure S2 in the supporting information). Although the variations are less pronounced when using the *Anand et al.* [2003] calibration equations, the trend in both upper thermocline temperature variability and the ΔT estimates remain the same over the past 2000 years (Figure S2 in the supporting information). Therefore, the choice of the calibration equation for *P. obliquiloculata* does not affect our interpretation of upwelling intensity changes off southern Indonesia over the past 2000 years.

The *G. bulloides* Mg/Ca-based temperature record and its interpretation as an upwelling indicator are corroborated by the $\Delta T_{G.\ bulloides\text{-}P.obliquiloculata}$ estimates ($r = 0.59$ with 95% confidence interval (0.39; 0.65)). A higher thermal gradient (ΔT°C) between 0 to 700 C.E. and 900 to 1300 C.E. suggests a deeper thermocline off southern Indonesia compared to the late twentieth century, indicating reduced upwelling strength (Figure 2c). A smaller temperature difference occurs between ~ 750–900 C.E. and 1400–1850 C.E., indicating a shallower thermocline and increased upwelling intensity during these periods compared to the late twentieth century.

The relative abundances of mixed layer- and thermocline-dwelling species corroborate our main findings. The mixed layer-dwelling species decrease remarkably in abundance between ~ 1400 and 1850 C.E., while the thermocline-dwelling species display an opposite trend indicating that the depth of thermocline decreased during this period (Figures 2d and 2e). The trends in the relative abundance of mixed layer-dwelling species are similar to the $\Delta T_{G.\ bulloides\text{-}P.obliquiloculata}$ estimates ($r = 0.46$ with 95% confidence interval (0.29; 0.61)) and *G. bulloides* Mg/Ca-based temperature estimates ($r = 0.56$ with 95% confidence interval (0.42; 0.63)). Lower relative abundances of mixed layer-dwelling species around ~ 700–900 C.E. and ~ 1400–1850 C.E. are associated with a lower thermal ($\Delta T_{G.bulloides\text{-}P.obliquiloculata}$) gradient and lower *G. bulloides* Mg/Ca-based temperature estimates suggesting a shallower thermocline and increased upwelling (Figure 2).

3.2. Controls on Changes in Upwelling Intensity Over the Past 2000 Years

In order to identify factors controlling changes in upwelling intensity off southern Indonesia over the past two millennia, we compare our austral winter upwelling records with East Asian summer monsoon (EASM) rainfall reconstructions reflecting the same seasonal window (boreal summer/austral winter; Figure 3c). Provided that the cross-equatorial winds over the Indian Ocean connect the monsoon systems of both hemispheres, we would expect coherent changes in the strengths of the different monsoon subsystems. For that reason, we compare our *G. bulloides* Mg/Ca-based temperature record representing austral winter upwelling and hence the strength of Australian-Indonesian winter monsoon winds with a record of EASM variability. The comparison reveals that changes in upwelling off southern Indonesia over the last two millennia are negatively correlated with variations in EASM rainfall as recorded in Wanxiang Cave [*Zhang et al.*, 2008], subtropical China ($r = -0.55$ with 95% confidence interval (-0.63;-0.29)). We find that periods of enhanced upwelling and thus more intense austral winter monsoon winds over southern Indonesia are associated with decreased EASM rainfall over north/central China during the last 2000 years (Figure 3), a feature also detected by comparing the two monsoon systems on millennial timescales [*Mohtadi et al.*, 2011a].

Our finding of more intense austral winter monsoon winds over southern Indonesia and drier conditions over north/central China is consistent with modern observational records of atmospheric circulation and summer monsoonal rainfall [*Li and Li*, 2014]. These 40 year observational data sets have revealed that stronger low-level cross-equatorial winds over the Indonesian/Australian region are associated with a weakening of the EASM rainfall in north/central China along with a weakening and east northward shift of the western Pacific subtropical high, a key ingredient of the EASM system [*Li and Li*, 2014]. Thus, we suggest that over the past 2000 years both stronger (weaker) upwelling off southern Indonesia and weaker (stronger) EASM rainfall are controlled by strengthened (weakened) large-scale Australian/Indonesian cross-equatorial boreal summer/austral winter winds.

In modern climatology, variations in the strength of large-scale Australian/Indonesian cross-equatorial austral winter winds are highly sensitive to ENSO variability (see also above). *Susanto et al.* [2001] reported that upwelling along the coasts of southern Indonesia is not only locally forced by the alongshore winds associated with the SE monsoon but also remotely by atmosphere-ocean circulation changes associated with ENSO. During El Niño (La Niña) years, the upwelling strength off Java is increased (decreased) resulting in colder (warmer) surface water temperatures and a shallower (deeper) thermocline [*Susanto et al.*, 2005]. Likewise,

©2014. American Geophysical Union. All Rights Reserved.

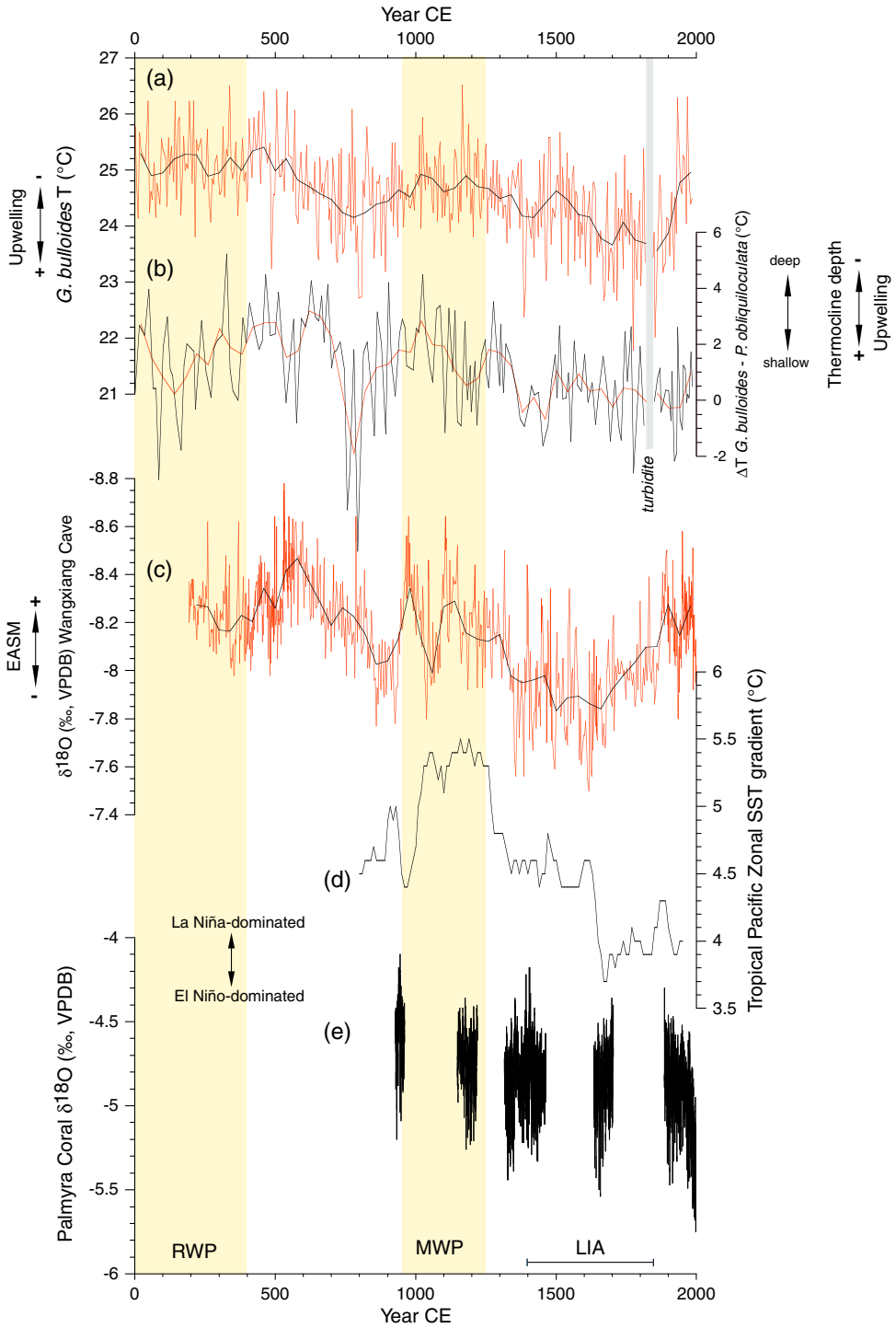

Figure 3. Comparison of the GeoB10065-7 upwelling records with other paleoclimate records for the last 2000 years. (a) Estimated temperatures derived from *G. bulloides* shell Mg/Ca ratios; (b) thermal gradient reconstructions ($\Delta T_{G.\ bulloides\ -\ P.\ obliquiloculata}$); (c) speleothem $\delta^{18}O$ of Wanxiang Cave, China [*Zhang et al.*, 2008]; (d) tropical Pacific zonal SST gradient [*Conroy et al.*, 2010]; and (e) Palmyra Island coral $\delta^{18}O$ in the central equatorial Pacific [*Cobb et al.*, 2003]; records of Figures 3a–3c were averaged in 10 year overlapping 50 year bins. Yellow bars indicate warm northern European/North Atlantic climate anomalies: Roman Warm Period (RWP) and Medieval Warm Period (MWP). LIA: Little Ice Age.

©2014. American Geophysical Union. All Rights Reserved.

western Pacific surface temperatures exert a significant control on the EASM as well, with higher (lower) surface temperatures during La Niña (El Niño) years leading to an earlier and stronger monsoon [*Jourdain et al*., 2013; *Feng and Hu*, 2014]. We therefore hypothesize that changes in the background state of the tropical Pacific, so-called "El Niño-like" or "La Niña-like" conditions may have substantially contributed to the centennial-scale upwelling trends observed in our records for upwelling from the eastern Lombok Basin during the past 2000 years. Assuming that changes in upwelling in the study area are mainly forced by atmosphere-ocean circulation changes related to ENSO, our upwelling records suggest the prevalence of an El Niño-like mean state during the LIA and a La Niña-like mean state during the MWP and RWP (Figure 3). Our results are consistent with reconstructions of global surface temperature patterns by *Mann et al*. [2009], which find a tendency for El Niño-like conditions in the tropical Pacific during the LIA and La Niña-like conditions during the MWP, as well as with a coral-based SST reconstruction from Palmyra Island in the central equatorial Pacific [*Cobb et al*., 2003] (Figure 3e). In addition, zonal gradient reconstructions of the tropical Pacific SST also suggest El Niño-like conditions during the LIA and La Niña-like conditions during the MWP (see Figure 3d) [*Conroy et al*., 2010]. As noted above, modern interannual variability in upwelling is not only strongly correlated with ENSO, but also with the IOD. The remarkable resemblance of our records for changes in upwelling with coral-based SST reconstruction in the central equatorial Pacific [*Cobb et al*., 2003] and zonal gradient reconstructions of the tropical Pacific SST [*Conroy et al*., 2010] suggests that ENSO has substantially contributed to the centennial-scale upwelling variations off southern Indonesia during the past 2000 years. As ENSO and IOD partly co-occur [e.g., *Behera et al*., 2006], we cannot rule out the contribution of IOD on the centennial-scale variations in upwelling off southern Indonesia. Due to the lack of independent proxy records for changes in the IOD over the past 2000 years, however, the influence of IOD on the variations in upwelling off southern Indonesia cannot be resolved conclusively yet.

Like in modern climatology [*Susanto et al*., 2001], our data for the past 2000 years thus seem to indicate a close relationship between changes in upwelling and ENSO (see above). As noted above, periods of stronger (weaker) upwelling and thus intensified (weakened) Australian/Indonesian cross-equatorial boreal summer/austral winter winds correspond to decreased (increased) EASM rainfall. The link to ENSO might also explain the close relationship between changes in upwelling off southern Indonesia and variations in EASM rainfall. In this context, observational records of precipitation and SST for the past 50 years reveal that in years, when SSTs in the central and eastern tropical Pacific are abnormally warm (= El Niño-like conditions), EASM circulation is weak which results in less summer precipitation over north/central China [*Yang and Lau*, 2004; *Feng and Hu*, 2014]. At the same time, SSTs are decreased in the eastern Indian Ocean [*Yang and Lau*, 2004]. In addition, modern observational data sets have further shown that the Australian/Indonesian cross-equatorial winds are intensified (weakened) during an El Niño (La Niña) episode [*Li and Li*, 2014]. Based on the instrumental records, the following scenario for changes in upwelling off southern Indonesia over the past 2000 years is proposed: stronger upwelling off southern Indonesia and thus intensified Australian/Indonesian cross-equatorial winds during the LIA might suggest an El Niño-like mean state whereas weaker upwelling off southern Indonesia and weaker cross-equatorial winds during the MWP and RWP indicate more La Niña-like dominated conditions. Our results are consistent with the findings of *Cobb et al*. [2003]; *Mann et al*. [2009] and *Khider et al*. [2011] which find more El Niño-like conditions in the tropical Pacific during the LIA and La Niña-like conditions during the MWP.

4. Conclusions

Our high-resolution records of upper water temperature, upper water column thermal structure, and relative abundances of mixed layer- and thermocline-dwelling planktonic foraminiferal species offshore northwest Sumba Island (southern Indonesia) reveal that upwelling was generally strong during Europe's LIA and weak during the MWP, as well as during the RWP. Our data reveal an inverse relationship between upwelling off southern Indonesia and EASM rainfall over the past 2000 years, consistent with modern (observed) modes of interannual variability. It appears that changes in the background state of the tropical Pacific, so-called El Niño-like or La Niña-like conditions may have substantially contributed to the centennial-scale upwelling variations as inferred from our records off southern Indonesia during the past two millennia. Our results further implicate the prevalence of an El Niño-like mean state during the LIA and a La Niña-like mean state during the MWP and the RWP. In addition, the potential influence of the IOD on the upwelling dynamics off southern Indonesia over the last 2000 years requires further investigations.

During the twentieth century, upwelling off southern Indonesia shows a decreasing trend. Accordingly, local austral winter near-surface ocean temperatures are high during the late twentieth century, but not

©2014. American Geophysical Union. All Rights Reserved.

unprecedented during the past 2000 years. SST reconstructions from the Moroccan Margin and Benguela upwelling systems, however, reveal an unprecedented cooling during the twentieth century that is interpreted to reflect increased upwelling, most likely linked to anthropogenic global warming [*McGregor et al*., 2007; *Leduc et al*., 2010]. The contrasting patterns of twentieth century upwelling development underline the importance to reconstruct the spatiotemporal patterns of past climate variability in order to better understand the influence of natural and anthropogenic forcings on the global climate system [*PAGES 2 K Consortium*, 2013].

Acknowledgments

We are grateful to S. Pape for technical support and K.B. Olafsdottir for statistical analyses. S. Steinke and M. Mohtadi acknowledge financial support from the Deutsche Forschungsgemeinschaft (DFG grants STE1044/4-1 and HE3412/15-1) and the German Ministry of Education and Research (BMBF grant PABESIA). The data in this study are archived and can be retrieved at PANGAEA (Publishing Network for Geoscientific and Environmental Data).

Peter Strutton thanks two anonymous reviewers for their assistance in evaluating this paper.

References

Anand, P., H. Elderfield, and M. H. Conte (2003), Calibration of Mg/Ca thermometry in planktonic foraminifera from a sediment trap time series, *Paleoceanography*, *18*(2), 1050, doi:10.1029/2002PA000846.

Barker, S., M. Greaves, and H. Elderfield (2003), A study of cleaning procedures used for foraminiferal Mg/Ca paleothermometry, *Geochem. Geophys. Geosyst.*, *4*(9), 8407, doi:10.1029/2003GC000559.

Behera, S. K., J. J. Luo, S. Masson, S. A. Rao, H. Sakuma, and T. Yamagata (2006), A CGCM study on the interaction between IOD and ENSO, *J. Clim.*, *19*, 1688–1705.

Carton, J. A., and B. J. Giese (2008), A reanalysis of ocean climate using simple ocean data assimilation (SODA), *Mon. Weather Rev.*, *136*, 2999–3017, doi:10.1175/2007MWR1978.1.

Cléroux, C., E. Cortijo, P. Anand, L. Labeyrie, F. Bassinot, N. Caillon, and J.-C. Duplessy (2008), Mg/Ca and Sr/Ca ratios in planktonic foraminifera: Proxies for upper water column temperature reconstruction, *Paleoceanography*, *23*, PA3214, doi:10.1029/2007PA001505.

Cobb, K. M., C. D. Charles, H. Cheng, and R. L. Edwards (2003), El Nino/Southern Oscillation and tropical Pacific climate during the last millennium, *Nature*, *424*, 271–276.

Conroy, J. L., J. T. Overpeck, and J. E. Cole (2010), El Niño/Southern Oscillation and changes in the zonal gradient of tropical Pacific sea surface temperature over the last 1.2 ka, *PAGES news*, *18*, 32–34.

Elderfield, H., and G. Ganssen (2000), Past temperature and $\delta^{18}O$ of surface ocean waters inferred from foraminiferal Mg/Ca ratios, *Nature*, *405*, 442–445, doi:10.1038/35013033.

Feng, J., and D. Hu (2014), How much does heat content of the western tropical Pacific Ocean modulate the South China Sea summer monsoon onset in the last four decades?, *J. Geophys. Res. Oceans*, *119*, 4029–4044, doi:10.1002/2013JC009683.

Greaves, M., et al. (2008), Interlaboratory comparison study of calibration standards for foraminiferal Mg/Ca thermometry, *Geochem. Geophys. Geosyst.*, *9*, Q08010, doi:10.1029/2008GC001974.

Hendiarti, N., H. Siegel, and T. Ode (2004), Investigation of different coastal processes in Indonesian waters using SeaWiFS data, *Deep Sea Res. II*, *51*, 85–97.

Jourdain, N., A. Gupta, A. Taschetto, C. Ummenhofer, A. Moise, and K. Ashok (2013), The Indo-Australian monsoon and its relationship to ENSO and IOD in reanalysis data and the CMIP3/CMIP5 simulations, *Clim. Dyn.*, *41*, 3073–3102.

Khider, D., L. D. Stott, J. Emile-Geay, R. Thunell, and D. E. Hammond (2011), Assessing El Niño Southern Oscillation variability during the past millennium, *Paleoceanography*, *26*, PA3222, doi:10.1029/2011PA002139.

Leduc, G., C. T. Herbert, T. Blanz, P. Martinez, and R. Schneider (2010), Contrasting evolution of sea surface temperature in the Benguela upwelling system under natural and anthropogenic climate forcings, *Geophys. Res. Lett.*, *377*, L20705, doi:10.1029/2010GL044353.

Li, C., and S. Li (2014), Interannual seesaw between the Somali and the Australian cross-equatorial flows and its connection to the East Asian summer monsoon, *J. Clim*, *27*, 3966–3980, doi:10.1175/JCLI-D-13-00288.1.

Locarnini, R. A., A. V. Mishonov, J. I. Antonov, T. P. Boyer, H. E. Garcia, O. K. Baranova, M. M. Zweng, and D. R. Johnson (2010), *World Ocean Atlas 2009, Volume 1: Temperature*, NOAA Atlas NESDIS 68, edited by S. Levitus, 184 pp., U.S. Gov. Print. Off., Washington, D. C.

Mann, M. E., Z. Zhang, M. K. Hughes, R. S. Bradley, S. K. Miller, S. Rutherford, and F. Ni (2008), Proxy-based reconstructions of hemispheric and global surface temperature variations over the past two millennia, *Proc. Natl. Acad. Sci. U.S.A.*, *105*, 13,252–13,257, doi:10.1073/PNAS0805721105.

Mann, M. E., Z. Zhang, S. Rutherford, R. S. Bradley, M. K. Hughes, D. Shindell, C. Ammann, G. Faluvegi, and F. Ni (2009), Global signatures and dynamical origins of the Little Ice Age and Medieval Climate Anomaly, *Science*, *326*, 1256–1260, doi:10.1126/science.1177303.

Masson-Delmotte, V., et al. (2013), Information from paleoclimate archives, in *Climate Change 2013: The Physical Science Basis*, Contribution of Working Group I to the Fifth Assessment Report of the Intergovernmental Panel on Climate Change, edited by T. F. Stocker et al., pp. 383–464, Cambridge Univ. Press, Cambridge, U. K., and New York.

McGregor, H. V., M. Dima, H. W. Fischer, and S. Mulitza (2007), Rapid 20th-century increase in coastal upwelling off Northwest Africa, *Science*, *315*, 637–639, doi:10.1126/science.1134839.

Mohtadi, M., L. Max, D. Hebbeln, A. Baumgart, N. Krück, and T. Jennerjahn (2007), Modern environmental conditions recorded in surface sediments samples off W and SW Indonesia: Planktonic foraminifera and biogenic compounds analyses, *Mar. Micropal.*, *65*, 96–112, doi:10.1016/j.marmicro.2007.06.004.

Mohtadi, M., S. Steinke, J. Groeneveld, H. G. Fink, T. Rixen, D. Hebbeln, B. Donner, and B. Herunadi (2009), Low-latitude control on seasonal and interannual changes in planktonic foraminiferal flux and shell geochemistry off south Java: A sediment trap study, *Paleoceanography*, *24*, PA1201, doi:10.1029/2008PA001636.

Mohtadi, M., D. W. Oppo, S. Steinke, J.-B. Stuut, R. De Pol-Holz, D. Hebbeln, and A. Lückge (2011a), Glacial to Holocene swings of the Australian-Indonesian monsoon, *Nat. Geosci.*, *4*, 540–544, doi:10.1038/NGEO1209.

Mohtadi, M., D. W. Oppo, A. Lückge, R. DePol-Holz, S. Steinke, J. Groeneveld, N. Hemme, and D. Hebbeln (2011b), Reconstructing the thermal structure of the upper ocean: Insights from planktic foraminifera shell chemistry and alkenones in modern sediments of the tropical eastern Indian Ocean, *Paleoceanography*, *26*, PA3219, doi:10.1029/2011PA002132.

Mohtadi, M., M. Prange, D. W. Oppo, R. De Pol-Holz, U. Merkel, X. Zhang, S. Steinke, and A. Lückge (2014), North Atlantic forcing of tropical Indian Ocean climate, *Nature*, *509*, 76–80, doi:10.1038/nature13196.

Ningsih, N. S., N. Rakhmaputeri, and A. B. Harto (2013), Upwelling variability along the Southern coast of Bali and in Nusa Tenggara Waters, *Ocean Sci. J.*, *48*, 49–57, doi:10.1007/s12601-013-0004-3.

Olaffsdottir, K. B., and M. Mudelsee (2014), More accurate, calibrated bootstrap confidence intervals for estimating the correlation between two time series, *Math. Geosci.*, *46*, 411–427, doi:10.1007/s11004-014-9523-4.

PAGES 2 k Consortium (2013), Continental-scale temperature variability during the past two millennia, *Nat. Geosci.*, *6*, 339–346, doi:10.1038/NGEO1797.

©2014. American Geophysical Union. All Rights Reserved.

Ravelo, A. C., R. G. Fairbanks, and S. G. H. Philander (1990), Reconstructing tropical Atlantic hydrography using planktonic foraminifera and an ocean model, *Paleoceanography*, *5*, 409–431, doi:10.1029/PA005i003p00409.

Sprintall, J., J. T. Potemra, S. L. Hautalac, N. A. Bray, and W. W. Pandoe (2003), Temperature and salinity variability in the exit passages of the Indonesian Throughflow, *Deep Sea Res. II*, *50*, 2183–2204.

Steinke, S., M. Mohtadi, J. Groeneveld, L.-C. Lin, L. Löwemark, M.-T. Chen, and R. Rendle-Bühring (2010), Reconstructing the southern South China Sea upper water column structure since the Last Glacial Maximum: Implications for the East Asian winter monsoon development, *Paleoceanography*, *25*, PA2219, doi:10.1029/2009PA001850.

Steinke, S., C. Glatz, M. Mohtadi, J. Groeneveld, Q. Li, and Z. Jian (2011), Past dynamics of the East Asian monsoon: No inverse behaviour between the summer and winter monsoon during the Holocene, *Global Planet. Change*, *78*, 170–177, doi:10.1016/j.gloplacha.2011.06.006.

Steinke, S., M. Mohtadi, M. Prange, V. Varma, D. Pittauerova, and H. W. Fischer (2014), Mid- to Late-Holocene Australian-Indonesian summer monsoon variability, *Quat. Sci. Rev.*, *93*, 142–154, doi:10.1016/j.quascirev.2014.04.006.

Susanto, R. D., and J. Marra (2005), Effects of the 1997/98 El Niño on Chlorophyll a variability along the southern coasts of Java and Sumatra, *Oceanography*, 18(4), 124–127, doi:10.5670/oceanog.2005.13.

Susanto, R. D., A. L. Gordon, and Q. Zheng (2001), Upwelling along the coasts of Java and Sumatra and its relation to ENSO, *Geophys. Res. Lett.*, *28*(8), 1599–1602, doi:10.1029/2000GL011844.

Susanto, R. D., T. S. Moore, and J. Marra (2006), Ocean color variability in the Indonesian Seas during the SeaWiFS era, *Geochem. Geophys. Geosyst.*, *7*, Q05021, doi:10.1029/2005GC001009.

Van der Plas, L., and A. C. Tobi (1965), A chart for judging the reliability of point counting results, *Am. J. Sci.*, *263*, 87–90.

Yang, F., and K.-M. Lau (2004), Trend and variability of China precipitation in spring and summer: Linkage to sea-surface temperatures, *Int. J. Climatol.*, *24*, 1625–1644.

Zhang, P., et al. (2008), A test of climate, sun, and culture relationships from an 1810-year Chinese cave record, *Science*, *322*, 940–942, doi:10.1126/science.1163965.

©2014. American Geophysical Union. All Rights Reserved.